ChemElectroChem

Research Article
doi.org/10.1002/celc.202300641

Chemistry Europe
European Chemical Societies Publishing

www.chemelectrochem.org

Electroanalytical Immunotool to Determine Matricellular Protein Periostin, a Stromal Biomarker of Prognosis in Colorectal Cancer

Marina Blázquez-García[+],[a] Jennifer Quinchia[+],[a, b] Víctor Ruiz-Valdepeñas Montiel,[a] Rebeca M. Torrente-Rodríguez,[a] Verónica Serafín,[a] María Garranzo-Asensio,[c] Ana García-Romero,[a, c] Jahir Orozco,[b] Rodrigo Barderas,[c] José M. Pingarrón,*[a] and Susana Campuzano*[a]

Tumor-associated stroma biomarkers are emerging as key signaling molecules of metastasis in colorectal cancer (CRC). In this sense, periostin (POSTN), a protein of the extracellular matrix from the stromal compartment, is envisioned as a potential stromal prognostic biomarker, which facilitates the application of pertinent treatments. In this work, we report an easy-to-handle amperometric sandwich-based immunosensing strategy for the determination of POSTN involving commercial magnetic microparticles (MBs), disposable carbon electrodes, and the horseradish peroxidase (HRP)/H_2O_2/hydroquinone (HQ) electrochemical system. The method allowed a dynamic linear range between 0.47 and 25 ng mL^{-1} and a limit of detection, LOD, of 0.14 ng mL^{-1} compatible with clinical demands. The method was applied to the analysis of POSTN in a variety of cancer-related real bio-scenarios including cell extracts and secretomes from CRC cells, and plasma from CRC patients at different stages. The potentials of this firstly developed MBs-assisted immunoplatform are justified by distinguishing between metastatic abilities of cultured CRC cells through the analysis of their extracts and secretomes, and by differentiating between healthy controls and CRC patients in just 60 min. Therefore, the developed immunoplatform can be envisaged as a novel and profitable tool for exploring the most uncharacterized but prospective tumor areas.

Introduction

For decades, surgery, radiation therapy, and chemotherapy have been the methods of choice for treating any type of cancer in patients without considering the unique features of tumors. Fortunately, we are witnessing an unprecedented revolution thanks to the recognition of the importance of precision medicine and the discovery of biomarkers, bodily-synthesized entities that provide bioinformation to detect, predict, diagnose, select therapy and stratify patients even at early stages.[1–3] Solid cancers contribute significantly to the world's highest mortality and overall health burden[4] with CRC ranking as the third most common diagnosed type of cancer and the second in global cancer-related deaths.[5] Importantly, patients suffering from distant metastasis showed an expected 5-year survival rate of less than 10%, which can reach 90% when CRC is detected at early stages.[6] It is known that not only cancer cells, but also the stromal compartment, formed by the non-malignant cells of the tumor (i.e., the tumor microenvironment), play important roles in CRC progression and metastasis. This compartment also includes an extracellular matrix (ECM) that is directly linked to the response to surgery, patient outcome, and oncologic therapy in CRC patients.[7,8] There is also increasing evidence that the role of ECM-derived proteins is decisive in inflammatory responses[9] and tumor development.[10] All this makes cancer researchers pay attention on both tumor microenvironment and ECM to understand the connection between tumor biology and cancer patients' medical history, thus improving personalized cancer treatments.[11]

The ingredients that make up the ECM include the protein periostin, also known as POSTN.[12] POSTN belongs to the matricellular proteins family, a class of extracellularly secreted non-structural ECM proteins that are normally expressed at low

[a] M. Blázquez-García,[+] J. Quinchia,[+] V. Ruiz-Valdepeñas Montiel, R. M. Torrente-Rodríguez, V. Serafín, A. García-Romero, J. M. Pingarrón, S. Campuzano
Department of Analytical Chemistry
Faculty of Chemistry
Complutense University of Madrid
Pza. de las Ciencias 2, 28040-Madrid (Spain)
E-mail: pingarro@quim.ucm.es
susanacr@quim.ucm.es

[b] J. Quinchia,[+] J. Orozco
Max Planck Tandem Group in Nanobioengineering, Institute of Chemistry
Faculty of Natural and Exact Sciences
University of Antioquia
Complejo Ruta N, Calle 67 No. 52–20, Medellín 050010 (Colombia)

[c] M. Garranzo-Asensio, A. García-Romero, R. Barderas
Chronic Disease Programme (UFIEC)
Instituto de Salud Carlos III
28220 Majadahonda, Madrid (Spain)

[+] The authors contributed equally to this work.

Supporting information for this article is available on the WWW under https://doi.org/10.1002/celc.202300641

levels in adult tissues,[13] while it is abnormally upregulated in various pathological events including tumor progression.[14]

A high expression of POSTN is usually associated with a more aggressive tumor, advanced stage, shorter overall survival rates and poor prognosis. Consequently, this protein is considered a useful biomarker for management of different cancer types[15–19] including CRC.[20,21] Delving into the second deadliest gastrointestinal malignancy worldwide, CRC, the prominent role and undeniable prognostic significance of POSTN have been shown in several recent research reports.[22] For example, Song et al. and Ben et al. found that POSTN was approximately 4-fold upregulated in CRC tissues and significantly elevated in serum from stratified advanced-stage[23] and preoperative[15] CRC patients, respectively, observing also implicit correlations between serum POSTN expression and clinical characteristics of colorectal tumors such as metastasis and disease progression.

Apart from the traditional methods of analysis, including LC–MS/MS and ELISA,[15,23] optical sensors and biosensors have been used to determine POSTN in biological specimens.[24–26] Surprisingly, and despite the advantageous characteristics of electrochemical biosensors in terms of versatility, cost, rapid detection, sensitivity and selectivity, possible miniaturization, field applicability, compatibility with multiplexed and/or multiomics determinations and coupling with a wide variety of micro and nanomaterials,[27,28] they have been sparsely employed for the determination of POSTN. To the best of our knowledge, only one electrochemical immunosensor using AuNPs decorated polydopamine/silica surfaces onto a glassy carbon electrode has been reported for POSTN determination. However, the method required more than 24 hours and was applied to help in the diagnosis of coronary artery disease.[29] The analysis of highly complex cancer-derived bio-matrices ideally demands the employment of suitable surfaces on which to assemble the biosensing strategy, thus ensuring reproducible results. In this sense, magnetic microparticles (MBs) offer a vast number of advantages (improved kinetics and efficiency of affinity reactions, easy handling, large surface area and abundant groups for biofunctionalization, among others[30–33]) over other types of materials to develop biosensing tools capable of fulfilling the expected features for these highly challenging applications. Therefore, both the relevance of POSTN as a prognostic biomarker for CRC and the absence of electrochemical biosensors involving MBs for the determination of POSTN in cancer-related bio-scenarios, led us to implement the first MBs-assisted amperometric immunoplatform for this protein and to apply it to the analysis of extracts and secretomes of cultured CRC cells with different metastatic potential, as well as to analyze plasma samples of diagnosed CRC patients at different stages.

Results and Discussion

The setup configuration of the sandwich-type immunosensing platform developed for the determination of POSTN, involving specific antibodies, magnetic microparticles and amperometric transduction, is illustrated in Scheme 1. Briefly, and according to the experimental procedures described in Section "Biofunctionalization of Magnetic Microparticles", the immunocaptors were first assembled by covalent immobilization of the capture antibody (CAb) onto carboxylic magnetic microparticles (HOOC-MBs). Thereafter, a sandwich-type immunoassay configuration was employed for the single-step detection of the target protein involving the incubation of the CAb-MBs with a mixture of human POSTN, biotinylated detector antibody (b-DAb) and a polymer of streptavidin conjugated to horseradish peroxidase (Strep-HRP) as an enzymatic tracer. The resulting MBs were placed on the surface of the working electrode of screen-printed electrodes (SPCEs) previously placed on a lab made polymethylmethacrylate casing with a built-in Nd magnet located underneath the surface of the working electrode. The affinity immunoreactions were monitored by amperometry transduction at −0.20 V (vs. Ag. pseudo-refence electrode) in stirred solutions using the HRP/H_2O_2/HQ system which gave cathodic current variations dependent on the amount of HRP molecules immobilized on the modified MBs, in turn directly related with the POSTN concentration.

Optimization of the Experimental Variables Involved in the Immunoplatform Assembly

To develop the immunoplatform with the demanding characteristics of sensitivity and selectivity that the determination of POSTN requires, and in terms of simplicity and assay time, a judicious univariate optimization of the parameters involved in the immunoplatform assembly was carried out. The amperometric detection was carried out under the experimental conditions optimized in previous works using the same electrochemical system and disposable transducers.[34,35] Larger ratio values between the amperometric currents measured in the presence of 10 (S) or 0.0 ng mL^{-1} (B) POSTN standards were the selection criterion (signal-to-blank, S/B), to achieve the above-mentioned characteristics. The optimization results are shown in Figure S1 (in the Supporting Information), and Table 1 summarizes all the variables tested as well as the values selected for further work.

Effective and sensitive target protein trapping requires the rigorous optimization of the variables involved in the immunocaptors assembly. Therefore, the CAb concentration was first optimized. Figure S1a shows that the specific amperometric

Table 1. Experimental variables tested and selected values involved in the fabrication of the immunoplatform for the amperometric determination of POSTN.

Variable	Tested range	Selected value
[CAb] (μg mL^{-1})	0.0–100.0	50.0
CAb incubation time (min)	15–90	45
Sandwich protocol	A–D	D
[b-DAb] (μg mL^{-1})	0.0—5.0	1.0
Strep-HRP dilution	1/5000–1/250	1/1000
Analysis time (min)	15–120	60

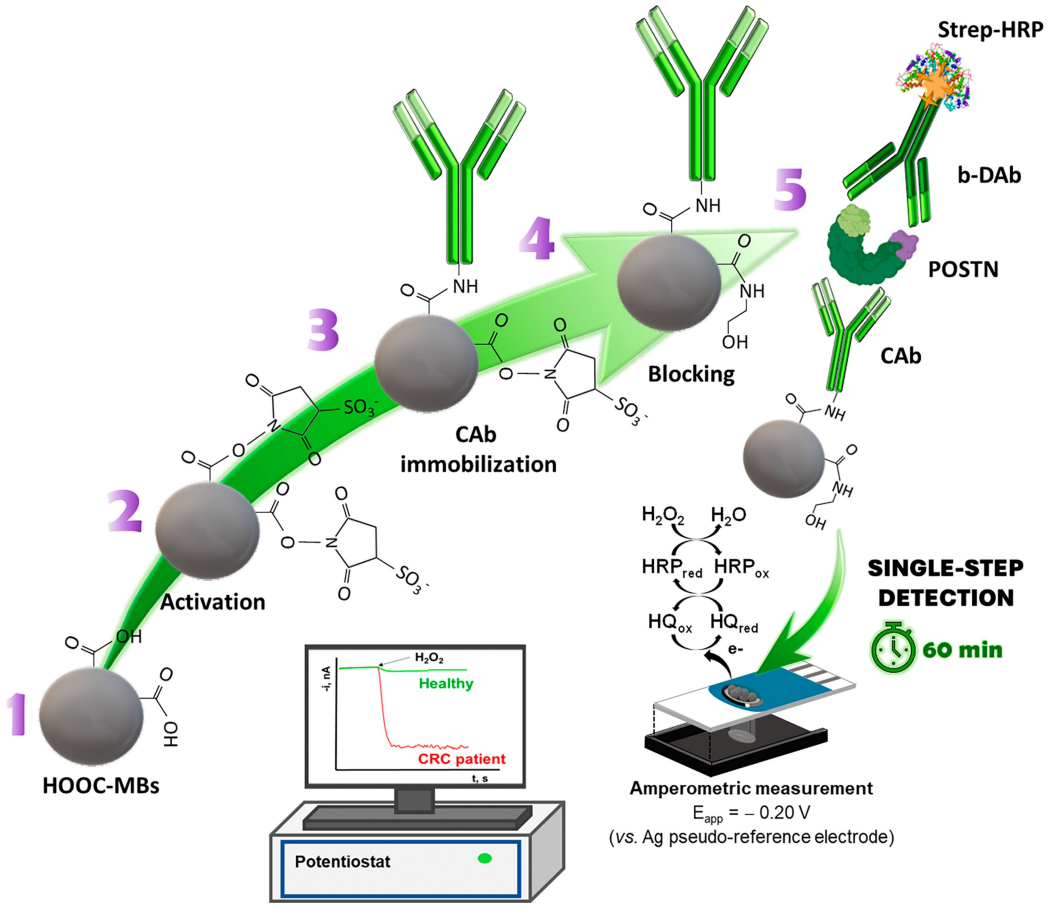

Scheme 1. Schematic display of the sandwich-type amperometric immunoplatform developed for the determination of human POSTN assisted by MBs.

signals measured in the presence of POSTN increased with the CAb concentration up to 50 μg mL^{-1}, while that signal decreased for larger concentrations, probably due to the restricted analyte accessibility to the CAb-binding sites for high amounts of immobilized antibody.[36,37]

In contrast, no significant effect was observed for the signals measured in the absence of the target protein (Figure S1a, white bars, B), indicating the absence of cross-reactivity between the pair of antibodies. Therefore, a larger S/B ratio was obtained for a 50 μg mL^{-1} CAb concentration which was selected for further experiments. The poor signal obtained in the absence of immobilized CAb (Figure S1a, "bars 0") confirmed the feasibility of the sandwich immunoassay. As shown in Figure S1b, 45 minutes were enough to ensure the efficient covalent immobilization of the CAb onto the activated HOOC-MBs. The observed decrease of the S/B ratio for longer immobilization times agreed with the results obtained with large CAb concentrations, due to the hindering of the antigen-antibody interaction.[38]

With the aim to implement a simple and rapid POSTN analysis protocol with minimal handling, the number of steps involved in the building of the HRP-labelled sandwich immunocomplexes on CAb-MBs was optimized. Four different protocols whose details are summarized in Table S1 (in the Supporting Information) were compared. All these protocols started from the CAb-MBs and involved successive incubation steps with single or mixed immunoreagent solutions.

As it can be seen in Figure S1c, a larger S/B ratio resulted when the assembly of the immunosensor was performed in a single step (protocol D). Since in all the tested protocols the non-specific adsorptions of the bioreagents are poor and similar (Figure S1c, white bars, B), this result can be attributed to the improvement of immunological recognition events and enzymatic labelling when they were carried out in homogeneous solutions. Therefore, Protocol D was selected to develop a "single incubation sample-to-result" analytical method. The optimization of the b-DAb concentration illustrated in Figure S1d showed a dramatic increment of the amperometric responses in the presence of POSTN and of the resulting S/B ratio up to 1 μg mL^{-1}, which was selected for subsequent experiments. The responses decrease observed for higher concentrations may be attributed to the less efficient recognition of the target under these conditions. Figure S1e shows the specific current measured in the presence of POSTN and the resulting S/B ratio increased with a lower dilution of the Strep-HRP conjugate up to 1/1000, falling sharply for larger concentrations (lower dilutions) of Strep-HRP. This behavior can be attributed to the four-fold multivalency of streptavidin, which can cause cross-reaction of a single streptavidin conjugate molecule with multiple b-DAbs, resulting in a lower number of

enzymatic units attached to the MBs.[39–41] Therefore, a 1000-fold dilution of Strep-HRP was selected for further work. Finally, 60 min was selected as the time to assemble the HRP-labelled sandwich immunocomplexes on CAb-MBs by incubation of the latter with the mixture solution containing POSTN, b-DAb and Strep-HRP (Figure S1f).

Analytical Performance and Operational Characteristics of the Immunoplatform

Once optimized the experimental variables, the analytical and operational characteristics of the immunoplatform developed for the determination of POSTN were evaluated. The calibration plot constructed with increasing concentrations of POSTN standards (Figure 1) exhibited a linear dependence of the measured cathodic current with the target protein concentration between 0.47 and 25 ng mL^{-1} (r = 0.9993), with slope and intercept values of (119 ± 2) nA mL ng^{-1} and (162 ± 21) nA, respectively. The LOD and limit of quantification, LOQ, estimated as described in Section "Data analysis" were 0.14 and 0.47 ng mL^{-1} (3.5 and 12 pg in the 25 μL incubation volume), respectively.

A comprehensive comparison of the analytical characteristics exhibited by the developed immunoplatform with those claimed for other reported bioassays is made in Table S2 (in the Supporting Information), as well as for commercial ELISA kits in Table S3 (in the Supporting Information). The LOD achieved with the developed immunoplatform is, in general, lower than those reported for optical,[15,24–26] chemiluminescent[42] and electrochemiluminescent[43] methods. In addition, it is of the same order as those claimed for commercial sandwich ELISA spectrophotometric kits (LODs ranging from 0.021 to 1.56 ng mL^{-1}, or 2.1–156 pg in the 100 μL incubation volume). However, the requirement of benchtop instrumentation restricts its use to remote and resource-constrained settings. To the best of our knowledge, only a label-free electrochemical immunosensor which involved AuNPs decorated polydopamine/silica surfaces onto non-disposable glassy carbon electrode and cyclic voltammetry transduction, has been reported.[29] The method achieved a LOD of 0.06 ng mL^{-1}, but the complex architecture required more than 24 hours of preparation. Moreover, its use for cancer monitoring was not verified. Although the LOD reached with the immunoplatform reported here is slightly higher than that reported by Zheng et al., the achieved sensitivity is sufficient to determine the concentration of POSTN in extracts of cultured cells, secretomes and in human plasma samples, where cut-off values for healthy individuals and patients diagnosed with CRC of 21.0 ± 7.3 and 47.2 ± 13.5 ng mL^{-1}, respectively, have been reported.[15] Also outstanding in state-of-the-art is the potential of the proposed methodology for timely off-benchtop analysis with an ease-of-use protocol involving a "single incubation sample-to-result" and amperometric transduction, the most widely implemented electrochemical detection technique in point-of-need devices, such as a glucometer.

The operational characterization of the proposed immunoplatform is another crucial aspect of its potential application and acceptance. First, the reproducibility in its fabrication was addressed by comparing the amperometric responses recorded for 2.5 ng mL^{-1} POSTN standard solutions with 10 different immunoplatforms prepared using the same protocol. A relative standard deviation (RSD) value of 4.3 %, was obtained indicating a high reproducibility of the entire experimental procedure, including the preparation of the immunocaptors (CAb-MBs), building of HRP-labelled sandwich immunocomplexes (HRP-Strep/b-DAb/POSTN/CAb/MBs) and their magnetic capture onto the SPCEs working electrode to perform the amperometric transduction. In addition, monitoring the amperometric responses for 0.0 (Figure S2 in the Supporting Information, empty circles) and 5 ng mL^{-1} of POSTN standards (Figure S2, full green circles) during various days using the CAb-MBs prepared on day 0 and stored at 4 °C in filtered PBS buffer, allowed us to evaluate their storage stability. As it can be seen in Figure S2,

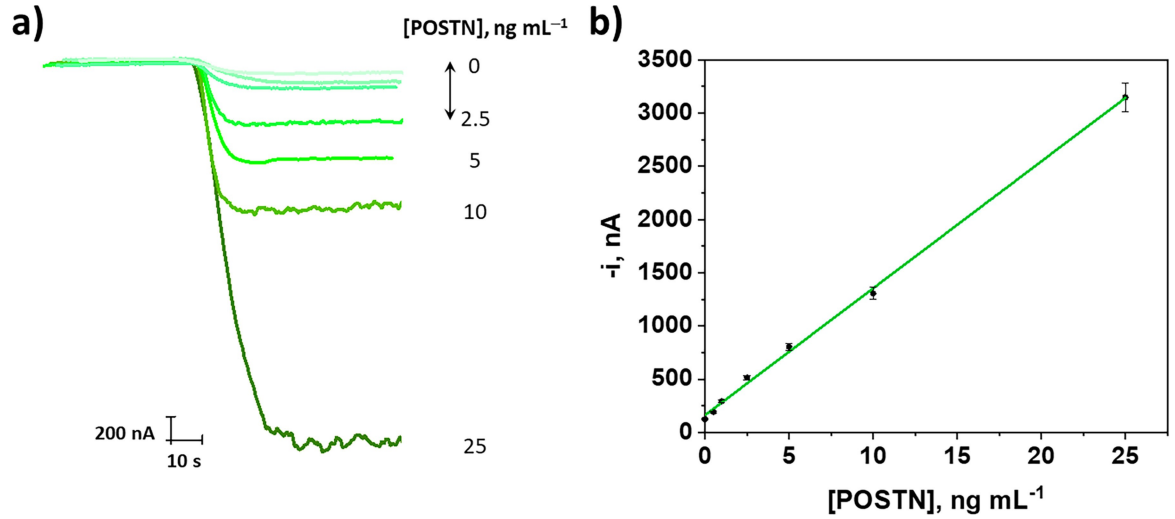

Figure 1. Real amperometric traces (a) and calibration plot (b) provided by the MBs-assisted immunoplatform for the determination of POSTN standards. In (b) error bars were estimated as the standard deviation (SD) of three replicates.

the amperometric responses were statistically comparable to those provided using the CAb-MBs prepared on the day 0 during at least 26 days (no longer times were evaluated), with the control limits set at ±3×SD (n = 3) of the measurements recorded on the day 0. Hence, batches of CAb-MBs can be manufactured, stored, and used for at least 26 days providing a similar sensitivity.

Selectivity of the Immunoassay

Although the design of single-step methodologies is the "dream" for point-of-care applications, reducing the number of assay steps may favor nonspecific adsorption to MBs and cross-reactive processes due to incubation of the sample with all the required bioreagents and the omission of intermediate washing steps. Therefore, to demonstrate that the simplicity of the methodology did not compromise its reliability, an exhaustive selectivity study was carried out by examining a selection of potentially interferent non-target proteins that might be present in biological specimens, such as circulating proteins (immunoglobulin G from human serum (hIgG), human hemoglobin (Hb), and human serum albumin (HSA)) and cancer-related biomarkers (human tumour necrosis factor-alpha protein (TNF), recombinant human cadherin-17 protein (CDH-17), recombinant human interleukin-13 receptor alpha 2 (IL13Rα2), and recombinant human T-cell immunoglobulin mucin domain 1 protein (TIM-1)). The amperometric measurements for 0.0 (B) and 2.5 (S) ng mL^{-1} POSTN, prepared in the absence and in the presence of each potential interfering compound at the concentrations typically found in serum, were recorded. The comparison between the different amperometric responses obtained in the absence of the target protein (Figure 2, white bars) demonstrates the absence of specific recognition between the immunoreagents and all the tested compounds except HSA. In fact, the interference from HSA has been widely reported in immunological tests and has been mainly attributed to the presence of hIgG in low-purity HSA lots, which could alter the test, especially when HSA is used at concentrations equal to or larger than 5 mg mL^{-1}.[44,45] The comparison of the S/B ratio values (Figure 2, red dots) also indicated significant interference of hIgG, Hb and TNF, while a negligible effect was observed in the presence of the other non-target proteins. The interference from hIgG can be attributed to the presence of circulating human antibodies reactive to mouse-expressed antibodies, as it is the case for the ones used for the development of the POSTN immunoplatform, which can lead to inaccurate measurements.[44,46–48] In the context of this study, it is important to mention that POSTN is involved in the activation of numerous signaling pathways and interacts with various membrane receptors and other stromal proteins.[49] For example, increased Hb content in tumours derived from POSTN-producing cells[50] and activation of POSTN cell expression with TNF[49,51] have been reported. Therefore, the interference observed in the presence of Hb and TNF may be due to these interactions. Moreover, although Hb has been widely reported to cause false positives due to its peroxidase activity, its prooxidant action can also lead to the destabilization of the biological structure of some proteins, which would justify the low sensitivity found for the detection of POSTN in the presence of 5 mg mL^{-1} Hb.[52]

Interestingly, a 10-fold dilution of these interfering compounds ("bars Dilution 1/10" in Figure 2) minimized such interfering effect.

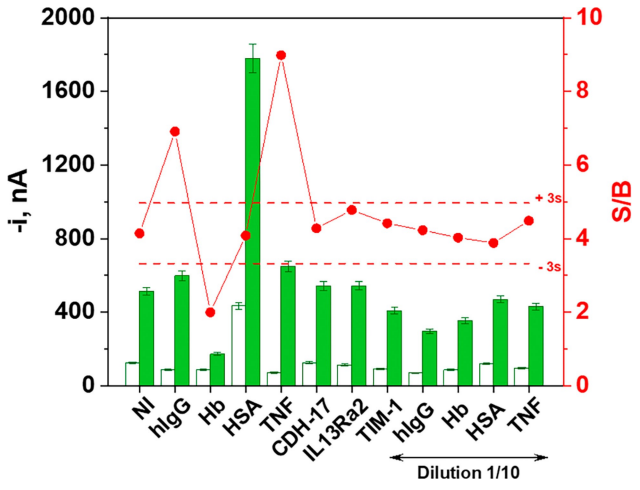

Figure 2. Amperometric responses measured with the developed immunoplatform for 0 (white bars, B) and 2.5 ng mL^{-1} POSTN (green bars, S) standard solutions prepared in the absence ("NI" bars) and in the presence of 1 and 0.1 mg mL^{-1} (1/10) hIgG; 5 and 0.5 mg mL^{-1} (1/10) Hb; 50 and 5 mg mL^{-1} (1/10) HSA; 10 and 1 ng mL^{-1} (1/10) TNF; 500 ng mL^{-1} CDH-17; 50 ng mL^{-1} IL13Rα2; and 2.5 ng mL^{-1} TIM-1. Control limits (red dashed lines) were set as 3×SD of the S/B mean value of three measurements obtained in the absence of interferent. Error bars were estimated as the SD of three replicates.

Analysis of Clinical Samples

The developed immunoplatform was then applied to the determination of POSTN in extracts and secretomes of cultured CRC cells with different metastatic capacities as well as in plasma from healthy individuals and patients diagnosed with CRC at different stages. Firstly, the presence of a matrix effect in these biological matrices was evaluated by comparing the slope values of the calibration plot constructed with POSTN standards prepared in the different matrices. Table S4 (in the Supporting Information) shows as, except for 5-times diluted SW480 secretome, there was a significant matrix effect in all the media tested.

Accordingly, the determination of POSTN in all the samples was carried out by applying the standard additions method with 1.0 μg of cell extract, 3-times (KM12C, KM12SM and KM12L4a) or 5-times (SW480 and SW620) diluted secretomes and 25-times diluted plasma samples.

The results obtained in the analysis of cellular samples are shown in Figure 3 and summarized in Table 2. As expected, a higher expression of the target protein was observed for both the extracts (Figure 3a) and secretomes (Figure 3b) of the isogenic pair metastatic cells. The semiquantitative results provided by the Western Blotting in the cell extracts (Figure 3c)

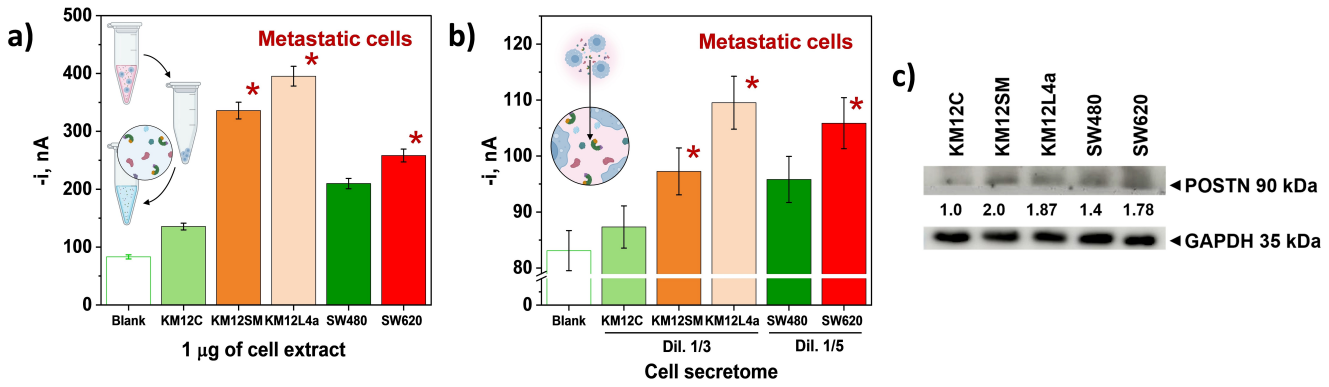

Figure 3. Results obtained with the developed immunoplatform for the determination of POSTN in cell extracts (a) and secretomes (b) from CRC cultured cells with different metastatic capacities. Western Blotting analysis in cell extracts (c), GAPDH was used as loading control, and protein signal intensities, quantified using the ImageJ software, were normalized according to expression in KM12C. In (a) and (b) error bars were estimated as the SD of three replicates.

Table 2. Results obtained with the developed immunoplatform for the determination of POSTN in extracts and secretomes of CRC cultured cells with different metastatic capacities.

	Extracts		Secretomes	
Cells	[POSTN] pg μg^{-1} [a]	$RSD_{n=3}$, %	[POSTN] ng mL^{-1} [a]	$RSD_{n=3}$, %
KM12C	3.9 ± 0.8	8.4	0.64 ± 0.04	2.7
KM12SM	13 ± 1	4.0	1.3 ± 0.1	4.6
KM12L4a	18 ± 1	3.4	2.2 ± 0.4	6.9
SW480	8 ± 1	5.0	1.6 ± 0.3	7.4
SW620	14 ± 2	4.9	5 ± 1	6.0

[a] Mean value ± ts/√n; n = 3; α = 0.05, t: Student's t value (two-tailed); s: standard deviation.[55]

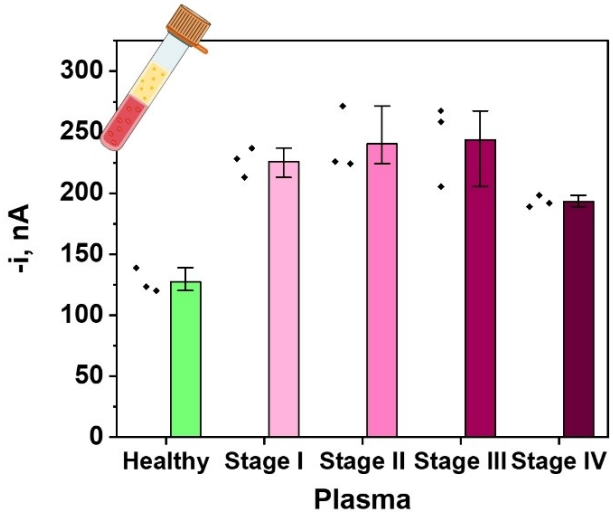

Figure 4. Amperometric readings obtained with the developed bioplatfom in plasma samples from a healthy individual and four patients with CRC in different stages. The values of the three replicates carried out for each sample are included in the representation. Error bars were estimated as the SD of three replicates.

Table 3. POSTN concentrations determined with the developed immunoplatform in plasma samples from a healthy individual and four patients with CRC at different stages.

Sample	[POSTN] ng mL^{-1} [a]	$RSD_{n=3}$, %
Healthy	15 ± 3	6.8
CRC (I)	43 ± 3	3.3
CRC (II)	51 ± 7	6.7
CRC (III)	60 ± 7	5.2
CRC (IV)	39.3 ± 0.2	0.2

[a] Mean value ± ts/√n; n = 3; α = 0.05.

agreed with those obtained with immunoplatforms (i.e., reduced levels of POSTN in non-metastatic KM12C and SW480 cell lines compared to their isogenic but metastatic counterparts KM12SM and KM12L4a, and SW620, respectively). However, due to lack of sensitivity, the usual blotting techniques (Western and Dot Blotting) were not able to detect POSTN in the cellular secretomes. Therefore, the high sensitivity of the developed methodology allowed us to provide the first quantitative data for POSTN in these cellular samples. In fact, the low concentrations for the target protein in the cell extracts (3.9–18 pg μg^{-1}) agreed with previous observations from the literature reporting that POSTN was mainly produced by the stromal cells surrounding the tumor, with CRC epithelial cells being negative or low in the production of POSTN.[13,15,53] It is important to mention that studies by Xiao et al.[54] confirmed the low expression of POSTN in SW480 cells and the role of POSTN in inducing chemoresistance to oxaliplatin or 5-fluorouracil in CRC cells. Therefore, these results support the potential of the developed immunoplatform not only for diagnosis and prognosis but also for therapeutic purposes.

Regarding the determination in plasma samples, the results displayed in Figure 4 and summarized in Table 3, showed, in agreement with that reported in the literature,[15,56] elevated POSTN concentrations in CRC patients compared to that of healthy volunteers. The measurements allowed a clear distinction between healthy controls and CRC patients although no association with clinical stages can be deduced probably due to the limited cohort of analyzed patients. Although discrepancies between the concentrations and the cut-off values of a given

biomarker in serum are usual, attributed to the use of different methods and different affinity of the antibodies employed, the levels found are in agreement with the described in the literature for healthy subjects: (21.0 ± 7.3) ng mL^{-1},[15] (20.4 ± 11.1) ng mL^{-1},[23] and (11.18 ± 5.51) ng mL^{-1} for >60 years and (12.29 ± 11.83) ng mL^{-1} for $\leq$ 60 years[57] and CRC patients: (40.9 ± 15.4) ng mL^{-1},[15] and (32.6 ± 10.8) ng mL^{-1}.[23] These results support the role of serum POSTN as a helpful serodiagnostic marker for CRC.[13,15,22,56,58,59]

Conclusions

This work reports the first electrochemical immunoplatform described for the determination of POSTN. The strategy implies the implementation of sandwich immunocomplexes and the use of MBs, SPCEs and HRP/H_2O_2/HQ redox system. This immunoplatform exhibited very attractive features, including high sensitivity (LOD = 0.14 ng mL^{-1}) and selectivity, short sample-to-answer time (60 min), simplicity (1 step), and low cost, which makes it competitive with existing biosensing methods for in-field applications. The immunoplatform has successfully tackled the analysis of extracts and secretomes of cultured CRC cells with different metastatic potential and of plasma samples from CRC patients at different stages. The quantitative results obtained highlight the potential of the target stromal biomarker to identify cells with metastatic potential and contribute to the diagnosis of patients with CRC. It is important to highlight that the immunoplatform, unlike conventional blotting technologies, does allow quantification in cellular samples, not only extracts but also in secretomes (where the lower concentrations do not allow the analysis with blotting techniques), also requiring smaller sample amounts and shorter testing times.

Additionally, unlike ELISA or immunoblotting technologies, due to the instrumentation and the type of transduction and transducers used, this immunoplatform has the potential to be used in multiplexed and/or point-of-need determination devices to advance the investigation of the tumor stroma and put in value the relevance of markers, such as POSTN, in the diagnosis, prognosis and oncological therapy.

Experimental Section

Apparatus and Electrodes

A CHI812B potentiostat (CH Instruments, Inc.) controlled by the CHI812B software was used to perform the amperometric measurements at room temperature. SPCEs (DRP110, 4-mm Ø, WE geometric area 12.6 mm^2) and the corresponding cable connector (DRP-CAC) were purchased from Metrohm-DropSens. Homemade polymethylmethacrylate casing with embedded Nd magnet (AIMAN GZ) was used for reproducible capture of the resulting magnetic bioconjugates on the SPCE working electrode surface.

Other instruments required for the functionalization of MBs included a thermomixer MT100 constant temperature incubator shaker (Universal Labortechnik) for sequential incubation steps of the MBs under constant stirring conditions at a given speed and temperature, a Dynamag-2 Magnet magnetic concentrator (Invitrogen-ThermoFisher Scientific) to separate MBs from the buffered or sample media, a vortex (VELP Scientifica) to ensure homogenization of the solutions and a Basic 20+ (Crison) pH-meter.

Reagents and Solutions

All reagents employed were of the highest available analytical grade. HOOC-MBs (2.8 μm Ø, 2×10^9 beads mL^{-1}, Dynabeads™ M-270 carboxylic acid, Cat. No.: 14305D) were provided by InvitrogenTM Thermo Fisher Scientific. Different salts including potassium chloride (KCl), sodium chloride (NaCl), disodium hydrogen phosphate (Na_2HPO_4), sodium di-hydrogen phosphate hydrated ($NaH_2PO_4 \cdot 2H_2O$) and Tris-hydroxymethyl-aminomethane-HCl (Tris-HCl) were purchased from Scharlab and ethylenediaminetetraacetic acid (EDTA) from Merck. N-hydroxysulfosuccinimide (Sulfo-NHS), N-(3-dimethyl-aminopropyl)-N'-ethyl-carbodiimide hydrochloride (EDC-HCl), ethanolamine, streptavidin-horseradish peroxidase conjugate (Strep-HRP, 500 U mL^{-1}), hydrogen peroxide (H_2O_2) (30%, w/v) and HQ were from Sigma-Aldrich. 2-(N-morpholino)ethanesulfonic acid (MES) was from Gerbu Biotechnik. The commercial blocker™ casein solution (BB solution: phosphate-buffered saline (PBS) containing 1% w/v casein, pH 7.4) and NaOH were purchased from Thermo Fisher Scientific and Labkem, respectively.

Recombinant human periostin standard (POSTN), mouse anti-human POSTN capture antibody (CAb), and biotinylated mouse anti-human POSTN detector antibody (b-DAb) were purchased as the components of the human Periostin/OSF-2 DuoSet ELISA (Cat. No.: DY3548B, R&D Systems).

Immunoglobulin G from human serum (hIgG, Ref: I2511), human hemoglobin (Hb, Cat. No. H7379), and human serum albumin (HSA, Cat. No. A1653) were acquired from Sigma-Aldrich. Human tumour necrosis factor-alpha protein (TNF-α, R&D Systems, Cat. No. DY210), recombinant human cadherin-17 protein (CDH-17, OriGene Technologies, Inc, Ref: TP720740), recombinant human interleukin-13 receptor alpha 2 (IL13Rα2, R&D Systems, Cat. No. DY614), and recombinant human T-cell immunoglobulin and mucin domain 1 protein (TIM-1, R&D Systems, Cat. No. DY1750B) were selected and tested as potential interfering compounds.

The buffered media employed were: 0.025 M MES (pH 5.0), 0.01 M phosphate buffer saline (PBS) containing 137 mM NaCl and 2.7 mM KCl (pH 7.5), 0.1 M phosphate buffer solution (PB) (pH 8.0), 0.1 M Tris-HCl (pH 7.2) and 0.05 M phosphate buffer (PB) (pH 6.0). They were prepared in type I deionized water from a Millipore Milli-Q purification system (18.2 MΩ cm). Solutions of EDC-HCl/Sulfo-NHS mixture (50 mg mL^{-1} each) and ethanolamine (1.0 M) used for the activation and blocking steps of the HOOC-MBs were prepared in MES buffer (pH 5.0) and in PB solution (pH 8.0), respectively, while stock solutions of the redox probe (0.1 M HQ) and HRP enzyme substrate (0.1 M H_2O_2) were freshly prepared in 0.05 M PB (pH 6.0).

Biofunctionalization of Magnetic Microparticles

Sequential modification of HOOC-MBs, consisting of successive incubation steps at 25 °C and 950 rpm, was performed in 1.5-mL microcentrifuge tubes using 25 μL of the corresponding bioreagent solution. After each incubation step, the supernatant/excess of each bioreagent solution was removed from the MBs suspension by placing the microcentrifuge tube in a magnetic concentrator for 3 min, followed by several washing steps with 50 μL of the corresponding buffer solution. After washing, the supernatant was

removed as stated above and the next incubation step could be performed.

Biofunctionalization of MBs was accomplished by pipetting a 3 μL aliquot of the HOOC-MBs commercial suspension in a microcentrifuge tube followed by two washings (10 min each) with MES buffer. Subsequently, surface carboxylic groups were derivatized to a semi-stable amine-reactive ester by re-suspending the microparticles in EDC-HCl/Sulfo-NHS mixture solution for 35 min, followed by two washings with MES buffer. Next, the biorecognition element was covalently attached to the activated MBs by incubating 50 $\mu g\,mL^{-1}$ of the specific capture antibody (CAb) solution (prepared in MES) for 45 min. After two washings with the same buffer media, the remaining active sites of the CAb-MBs were blocked with a solution of ethanolamine for 60 min to avoid non-specific adsorptions from other bioreagents and/or sample biocomponents. After one washing with Tris-HCl buffer and two more with BB solution, the prepared CAb-MBs were stored at 4 °C in filtered PBS until use.

The sandwich immunoassay was implemented on the previously blocked CAb-MBs by incubating, for 60 min, a mixture solution containing the corresponding concentration of the POSTN standard (or the analyzed sample), 1.0 $\mu g\,mL^{-1}$ b-DAb and 1/1000 diluted Strep-HRP, in BB, thus taking place the simultaneous capture, recognition and enzymatic labelling of the target protein onto the surface of the functionalized MBs. The resultant HRP-Strep/b-DAb/POSTN/CAb/MBs immunoconjugates were washed twice with BB solution.

Amperometric Measurements

The HRP-labelled sandwich-type magnetic immunoconjugates were resuspended in 50 μL of 0.05 M PB and, after proper homogenization with a micropipette, reproducibly deposited on the working electrode surface of a SPCE, previously placed in a homemade polymethylmethacrylate housing containing an Nd magnet.

Next, the magnetic conjugates/SPCE/casing assembly was connected to the potentiostat using the appropriate cable and immersed into an electrochemical cell containing 10 mL of 0.05 M PB supplemented with 100 μL of a freshly prepared 0.1 M HQ solution under magnetic stirring. Thereafter, a constant potential (−0.20 V vs. Ag pseudo-reference electrode) was applied to the working electrode, and the resultant current intensity (in nA) was recorded over time (in seconds). When the background current was stabilized (≈100 s), 50 μL of a freshly prepared 0.1 M H_2O_2 solution was added to the electrochemical cell and the resulting cathodic current was recorded until the steady-state was reached. The used measurements were taken as the difference between the steady-state and background currents.

Analysis of Cellular and Plasma Samples

This study focused on CRC biomarker validation was approved by the Ethical Review Boards of the Instituto de Salud Carlos III and Hospital Universitario Clínico San Carlos. Plasma from a healthy individual and CRC patients were provided from the IdISSC biobank of the Hospital Clínico San Carlos after Ethical Committee approval (CEI PI 13_2020-v2) and stored at −80 °C until use. All individuals provided written informed consent for the use of their biological samples for research purposes, adhering to ethical principles outlined by Spain (LOPD 15/1999) and the European Union Fundamental Rights of the EU (2000/C364/01). All samples were handled and used anonymously accomplishing all the ethical issues. Experiments were performed in agreement with relevant guidelines and regulations of Hospital Universitario Clínico San Carlos, Instituto de Salud Carlos III and Universidad Complutense de Madrid.

Two isogenic CRC cell models with the same genetic background but different metastatic properties were analyzed. The isogenic poorly metastatic KM12C cells, highly metastatic to liver KM12SM cells and highly metastatic to liver and lung KM12L4a cells were obtained from I. Fidler's laboratory (MD Anderson Cancer Center). Isogenic low metastatic SW480 cells and highly metastatic to lymphatic nodes SW620 cells were from the American Type Culture Collection.[60,61] These cells were grown and their extracts and secretomes obtained as described previously.[62] The protein concentration in the extracts was determined using the tryptophan method.[63]

For comparative purposes the cell extracts were also analyzed by Western Blotting. To do this, 10 μg of protein extracts from KM12C, KM12SM, KM12L4a, SW480, and SW620 CRC cells without β-mercaptoethanol (non-reducing conditions) were run and separated in 10% SDS-PAGE before transference to nitrocellulose membranes at 100 V for 90 min. After blocking with 3% BSA in PBS-0.1% Tween (PBST), membranes were incubated overnight at 4 °C with primary antibodies at optimized dilutions in blocking buffer (1/1000 anti-GAPDH (Santa Cruz Biotechnology), 1/1000 anti-POSTN (R&D Systems)). After extensive washing with PBST, membranes were incubated with 1/1000 HRP-labelled secondary antibody (Sigma). Reactive proteins were visualized using Super-Signal West Pico PLUS Chemiluminescent Substrate (ThermoScientific) and bands were quantified using ImageJ software (version 1.53t) and GAPDH as loading control and for normalization purposes.

The possible existence of a matrix effect in analyzing these cellular and plasma samples with the immunoplatform was evaluated. As it has been discussed in detail in Section "Analysis of Clinical Samples", the presence of matrix effect was concluded in most of these samples and, therefore, the determination was carried out by applying the standard additions method using 1.0 μg of cell extracts, secretomes diluted 3 or 5 times, depending on the isogenic pair, and 25 times diluted plasma samples.

Data Analysis

The data were analyzed using Microsoft Excel and Origin software. Bar and dot plots in the manuscript represent the cathodic current mean resulting from three replicates and the error bars were estimated as the SD of these replicates. The LOD and LOQ values were calculated according to the $3\times s_b/m$ or $10\times s_b/m$ criterion, respectively, where s_b is the standard deviation of ten measurements recorded in the absence of POSTN and m is the slope value of the calibration graph constructed with POSTN standards. The relative standard deviation (RSD = (SD/mean)×100%) was used to calculate the variability. The confidence intervals were estimated using mean value ± $ts/\sqrt{n}$ ($n = 3$; $\alpha = 0.05$).[55] The Student's t-test was used to statistically compare slope values.[64]

Acknowledgements

The financial support of Grant PID2019-103899RB–I00 funded by MCIN/AEI/10.13039/501100011033, EU's Horizon 2020 funding programme (UCM's Specific Research Fund FEI-EU-22-08) and PI20CIII/00019 and PI23CIII/00027 grants from the AES-ISCIII Program co-founded by FEDER funds are gratefully acknowledged. J.Q. was founded by Minciencias, Mineducacion, MINCIT,

and ICETEX through the Program Ecosistema Cientifico Cod. FP44842-211-2018, project number 58536. J.O. thanks support from the University of Antioquia and the Max Planck Society through the cooperation agreement 566-1, 2014.

Conflict of Interests

The authors declare no conflict of interest.

Data Availability Statement

The data that support the findings of this study are available from the corresponding authors upon reasonable request.

Keywords: POSTN · Magnetic microparticles · Disposable carbon electrodes · Colorectal cancer · Plasma

[1] M. A. Tainsky, *BBA* **2009**, *1796*, 176–193.
[2] V. Das, J. Kalita, M. Pal, *Biomed. Pharmacother.* **2017**, *87*, 8–19.
[3] T. Muinao, H. P. D. Boruah, M. Pal, *Exp. Cell Res.* **2018**, *362*, 1–10.
[4] M. Pal, T, Muinao, H. P. D. Boruah, N. Mahindroo, *Biomed. Pharmacother.* **2022**, *146*, 112488.
[5] R. L. Siegel, N. S. Wagle, A. Cercek, R. A. Smith, A. Jemal, *Ca-Cancer J. Clin.* **2023**, *73*, 233–254.
[6] B. A. A. Martins, G. Fonseca de Bulhoes, I. N. Cavalcanti, M. M. Martins, P. Gonçalves de Oliveira, A. M. A. Martins, *Front. Oncol.* **2022**, *9*, 1284.
[7] S. Crotti, M. Piccoli, F. Rizzolio, A. Giordano, D. Nitti, M. Agostini, *J. Cell. Physiol.* **2017**, *232*, 967–975.
[8] F. Kai, A. P. Drain, V. M. Weaver, *Dev. Cell.* **2019**, *49*, 332–346.
[9] H. J. Riley, A. D. Bradshaw, *Anat. Rec.* **2020**, *303*, 1624–1629.
[10] N. V. Popova, M. Jücker, *Cancers (Basel).* **2022**, *14*, 238.
[11] S. Karlsson, H. Nyström, *Crit. Rev. Oncol. Hematol.* **2022**, *175*, 103712.
[12] A. Y. Liu, H. Zheng, G. Ouyang, *Matrix Biol.* **2014**, *37*, 150–156.
[13] S. Dorafshan, M. Razmi, S. Safaei, E. Gentilin, Z. Madjd, R. Ghods, *Cancer Cell Int.* **2022**, *22*, 315.
[14] K. Ratajczak-Wielgomas, P. Dziegiel, *F. Histochem. Cytobiol.* **2015**, *53*, 120–132.
[15] Q.-W. Ben, Z. Zhao, S.-F. Ge, J. Zhou, F. Yuan, Y.-Z. Yuan, *Int. J. Oncol.* **2009**, *34*, 821–828.
[16] P. V. Nuzzo, A. Rubagotti, L. Zinoli, F. Ricci, S. Salvi, S. Boccardo, F. Boccardo, *Cancer* **2012**, *12*, 625.
[17] L.-Z. Hong, X.-W. Wei, J.-F. Chen, Y. Shi, *Oncol. Lett.* **2013**, *6*, 1595–1603.
[18] P.-L. Sung, Y.-H. Jan, S.-C. Lin, C.-C. Huang, H. Lin, K.-C. Wen, K.-C. Chao, C.-R. Lai, P.-H. Wang, C.-M. Chuang, H.-H. Wu, N.-F. Twu, M.-S. Yen, M. Hsiao, C. Y. F. Huang, *Oncotarget* **2016**, *7*, 4036–4047.
[19] G.-E. Kim, J. S. Lee, M. H. Park, J. H. Yoon, *PLoS One* **2017**, *12*, e0187635.
[20] X. Xu, W. Chang, J. Yuan, X. Han, X. Tan, Y. Ding, Y. Luo, H. Cai, Y. Liu, X. Gao, Q. Liu, Y. Yu, Y. Du, H. Wang, L. Ma, J. Wang, K. Chen, Y. Ding, C. Fu, G. Cao, *Oncotarget* **2016**, *7*, 798–813.
[21] H. J. Oh, J. M. Bae, X.-Y. Wen, N.-Y. Cho, J. H. Kim, G. H. Kang, *J. Pathol. Transl. Med.* **2017**, *51*, 306–313.
[22] X. Deng, S. Ao, J. Hou, Z. Li, Y. Lei, G. Lyu, *Chin. J. Cancer Res.* **2019**, *31*, 547–556.
[23] L.-N. Song, L.-X. li, Q.-H. Shi, L. Fang, L. Sun, H.-F. Zhao, N. Liu, H.-J. Li, C.-Y. He, *Bangladesh J. Pharmacol.* **2014**, *9*, 488–495.
[24] M. Chatzipetrou, L. Gounaridis, G. Tsekenis, M. Dimadi, R. Vestering-Stenger, E. F. Schreuder, A. Trilling, G. Besselink, L. Scheres, A. van der Meer, E. Lindhout, R. G. Heideman, H. Leeuwis, S. Graf, T. Volden, M. Ningler, C. Kouloumentas, C. Strehle, V. Revol, A. Klinakis, H. Avramopoulos, I. Zergioti, *Sensors* **2021**, *21*, 2230.
[25] M. Scheres, *Chem. Sci.* **2022**, *13*, 300.
[26] J. Park, C. Ban, *Sci. Rep.* **2023**, *13*, 10224.
[27] J. H. Kim, Y. J. Suh, D. Park, H. Yim, H. Kim, H. J. Kim, D. S. Yoon, K. S. Hwang, *Biomed. Eng. Lett.* **2021**, *11*, 309–334.
[28] A. Singh, A. Sharma, A. Ahmed, A. K. Sundramoorthy, H. Furukawa, S. Arya, A. Khosla, *Biosensors* **2021**, *11*, 336.
[29] X.-F. Zheng, Y.-Y. Wang, L. Han, X.-C. Wang, S.-L. Zhao, H. Zou, *Int. J. Electrochem. Sci.* **2017**, *12*, 819–828.
[30] A. Molinero-Fernández, M. Moreno-Guzmán, M. A. López, A. Escarpa, *Biosensors* **2020**, *10*, 66.
[31] S. Ustuner, M. A. Lindsay, P. Estrela, *Sci. Rep.* **2021**, *11*, 19650.
[32] Y. Chang, Y. Wang, J. Zhang, Y. Xing, G. Li, D. Deng, L. Liu, *Biosensors* **2022**, *12*, 954.
[33] S. Fortunati, C. Giliberti, M. Giannetto, A. Bertucci, S. Capodaglio, E. Ricciardi, P. Giacomini, V. Bianchi, A. Boni, I. De Munari, R. Corradini, M. Careri, *Biosens. Bioelectron.: X* **2023**, *15*, 100404.
[34] M. Eguílaz, M. Moreno-Guzmán, S. Campuzano, A. González-Cortés, P. Yáñez-Sedeño, J. M. Pingarrón, *Biosens. Bioelectron.* **2010**, *26*, 517–522.
[35] F. Conzuelo, M. Gamella, S. Campuzano, D. G. Pinacho, A. J. Reviejo, M. P. Marco, J. M. Pingarrón, *Biosens. Bioelectron.* **2012**, *36*, 81–88.
[36] V. Pérez-Ginés, R. M. Torrente-Rodríguez, A. Montero-Calle, G. Solís-Fernández, P. Atance-Gómez, M. Pedrero, J. M. Pingarrón, R. Barderas, S. Campuzano, *Biosens. Bioelectron.: X* **2022**, *11*, 100192.
[37] C. Muñoz-San Martín, V. Pérez-Ginés, R. M. Torrente-Rodríguez, M. Gamella, G. Solís-Fernández, A. Montero-Calle, M. Pedrero, V. Serafín, N. Martínez-Bosch, P. Navarro, P. García de Frutos, M. Batlle, R. Barderas, J. M. Pingarrón, S. Campuzano, *Electrochem. Sci. Adv.* **2022**, *2*, e2100096.
[38] J. Quinchia, M. Blázquez-García, R. M. Torrente-Rodríguez, V. Ruiz-Valdepeñas Montiel, V. Serafín, R. Rejas-González, A. Montero-Calle, J. Orozco, J. M. Pingarrón, R. Barderas, S. Campuzano, *Talanta* **2024**, *267*, 125155.
[39] R. Miranda-Castro, N. de-los-Santos-Álvarez, M. J. Lobo-Castañón, *Electroanalysis* **2018**, *30*, 1229–1240.
[40] S. Campuzano, P. Yáñez-Sedeño, J. M. Pingarrón, *ChemElectroChem* **2019**, *6*, 60–72.
[41] E. Povedano, V. Ruiz-Valdepeñas Montiel, A. Valverde, F. Navarro-Villoslada, P. Yáñez-Sedeño, M. Pedrero, A. Montero-Calle, R. Barderas, A. Peláez-García, M. Mendiola, D. Hardisson, J. Feliú, J. Camps, E. Rodríguez-Tomàs, J. Joven, M. Arenas, S. Campuzano, J. M. Pingarrón, *ACS Sens.* **2019**, *4*, 227–234.
[42] N. M. Jeanblanc, P. M. Hemken, M. J. Datwyler, S. E. Brophy, T. S. Manetz, R. Lee, M. Liang, P. S. Chowdhury, R. Varkey, E. P. Grant, K. Streicher, L. Greenlees, K. Ranade, G. J. Davis, *Clin. Chim. Acta* **2017**, *464*, 228–235.
[43] S. Palme, R. H. Christenson, S. A. Jortani, R. E. Ostlund, R. Kolma, G. Kopal, R. P. Laubender, *Clin. Biochem.* **2017**, *50*, 139–144.
[44] S. E. F. Melanson, M. J. Tanasijevic, P. Jarolim, *Circulation* **2007**, *116*, e501–e504.
[45] B. Arévalo, M. Blázquez-García, A. Valverde, V. Serafín, A. Montero-Calle, G. Solís-Fernandez, R. Barderas, P. Yáñez-Sedeño, S. Campuzano, J. M. Pingarrón, *Bioelectrochemistry* **2022**, *146*, 108157.
[46] L. J. Kricka, *Clin. Chem.* **1999**, *45*, 942–956.
[47] J. Tate, G. Ward, *Clin. Biochem. Rev.* **2004**, *25*, 105–120.
[48] J. Bjerner, K. H. Olsen, O. P. Børmer, K. Nustad, *Clin. Biochem.* **2005**, *38*, 465–472.
[49] L. Yang, T. Guo, Y. Chen, K. Bian, *Cells* **2023**, *12*, 50.
[50] R. Shao, S. Bao, X. Bai, C. Blanchette, R. M. Anderson, T. Dang, M. L. Gishizky, J. R. Marks, X.-F. Wang, *Mol. Cell. Biol.* **2004**, *24*, 3992–4003.
[51] S. Amara, K. Lopez, B. Banan, S.-K. Brown, M. Whalen, E. Myles, M. T. Ivy, T. Johnson, K. L. Schey, V. Tiriveedhi, *Mol. Immunol.* **2015**, *64*, 26–35.
[52] J. Simoni, G. Simoni, C. D. Lox, S. D. Prien, G. T. Shires, *Anal. Chim. Acta* **1995**, *313*, 1–14.
[53] A. Ueki, M. Komura, A. Koshino, C. Wang, K. Nagao, M. Homochi, Y. Tsukada, M. Ebi, N. Ogasawara, T. Tsuzuki, K. Kasai, K. Kasugai, S. Takahashi, S. Inaguma, *Cancers* **2023**, *15*, 606.
[54] Z.-M. Xiao, X.-Y. Wang, A.-M. Wang, *Biotechnol. Appl. Biochem.* **2015**, *62(3)*, 401–406.
[55] J. N. Miller, J. C. Miller, Statistics and Chemometrics for Analytical Chemistry, 7th Ed, Pearson Education Limited, **2018**. ISBN-13: 9781292186740.
[56] D. Dong, L. Zhang, L. Jia, W. Ji, Z. Wang, L. Ren, R. Niu, Y. Zhou, *Clin. Lab.* **2018**, *64*, 973–981.
[57] L. Jia, G. Li, N. Ma, A. Zhang, Y. Zhou, L. Ren, D. Dong, *BMC Cancer* **2022**, *22*, 760.
[58] Z. Li, X. Zhang, Y. Yang, S. Yang, Z. Dong, L. Du, L. Wang, C. Wang, *Int. J. Mol. Sci.* **2015**, *16*, 12108–12118.

[59] H. Ma, J. Wang, X. Zhao, T. Wu, Z. Huang, D. Chen, Y. Liu, G. Ouyang, *Cell Rep.* **2020**, *30*, 793–806.
[60] K. Morikawa, S. M. Walker, J. M. Jessup, I. J. Fidler, *Cancer Res.* **1988**, *48*, 1943–1948.
[61] K. Morikawa, S. M. Walker, M. Nakajima, S. Pathak, J. M. Jessup, I. J. Fidle, *Cancer Res.* **1988**, *48*, 6863–6871.
[62] S. Tejerina-Miranda, M. Pedrero, M. Blázquez-García, V. Serafín, A. Montero-Calle, M. Garranzo-Asensio, A. Julio Reviejo, J. M. Pingarrón, R. Barderas, S. Campuzano, *Bioelectrochemistry* **2024**, *155*, 108571.
[63] J. R. Wisniewski, F. Z. Gaugaz, *Anal. Chem.* **2015**, *87*, 4110–4116.
[64] J. M. Andrade, M. G. Estévez-Pérez, *Anal. Chim. Acta* **2014**, *838*, 1–12.

Manuscript received: November 7, 2023
Revised manuscript received: November 28, 2023
Version of record online: December 22, 2023